ASME Winter Annual Meeting
December 1988, Chicago

# Human Machine Interaction via the Transfer of Power and Information Signals; Part II: Dynamic and Control Analysis

H. Kazerooni

Mechanical Engineering
University of Minnesota
Minneapolis, MN 55455 USA

## ABSTRACT

The work presented here is focused on the issues related to the dynamics and control in human machine interaction in the sense of power and information signals. The extender is defined as an active manipulator worn by a human to increase the "strength" of the human wearing it. The human body, in physical contact with the extender, exchanges information signals and power with the extender. General models for the human, the extender and the interaction between the human and the extender have been developed. Unstructured modeling was chosen in order to include all the dynamics in the systems, to avoid specific models. Small Gain Theorem (time domain) for the nonlinear systems and the Nyquist Criterion (frequency domain) for the linearly treated systems have been used for stability analysis of human machine interaction. The equivalence of the conditions for stability when the Small Gain Theorem is extended to the linear systems has been shown. The stability condition is verified in Part I of the paper on a single degree of freedom extender.

## 1. INTRODUCTION

The extender system consists of three main parts: the human arm, the extender, and the interaction between the human arm and the extender. Considering the extender as a set of rigid members, the dynamic behavior of an open-loop extender can be derived by a set of nonlinear differential equations via the Lagrangian or Eulerian approach [6,7]. However, there may be too many components in an extender so the rigid body dynamics is not sufficient for modeling. Actuators and sensors, for example, contribute to the dynamics of the extender. Usually the dynamics of the actuators and sensors are negligible when compared with the dynamics of the links of the extender. However, if hydraulic actuators are used to power the extender, then the dynamic behavior of the actuators may be a considerable factor which is integrated into the total dynamic behavior of the system. The objective is to develop an unstructured dynamic model that can represent the complete dynamic behavior of the extender in a very general form. This unstructured modeling focuses on the relationship between the input and output properties of the extender. The structured dynamic models such as first or second order transfer functions that represent the dynamic behavior of the components of the extender (e.g. actuators or sensors) have been avoided; these models generally lead to very specific stability conditions.

In modeling the human arm, we use the same style that we used in modeling the extender; the human arm is viewed as a dynamic system which produces an output in response to an input command. The intent is to develop an unstructured dynamic model for the human arm in terms of a mapping which contains all the possible dynamics involved in a particular maneuvering. The emphasis of the model is on the functional relationship between the dynamic input and output properties of the human arm. Therefore, we are less concerned with the internal structure of the components in the arm model. Thus the particular dynamics of nerve conduction, muscle

contraction and central nervous system processing are implicitly accounted for in constructing the dynamic model of the human arm.

Using the unstructured models of human and extender, the closed loop system is introduced. By closing the loop we mean that the interaction force between the human and the extender will be fed back and used as an input to the velocity controlled extender. The resulting extender velocity is due to two feedback loops. The first is a natural feedback loop between the human and extender. The second feedback loop is the controlled loop. The goal is to develop a class of compensators which will guarantee the stability of the system as a whole.

## 2. DYNAMIC BEHAVIOR OF THE EXTENDER

There is no intention to design a controller for the system of the human and the extender as a whole. This is not practical because human dynamic behavior varies from one person to the other as well as within the same person. A velocity control algorithm is chosen as the lowest level of control for the extender such that the extender is able to follow various velocity commands in a cartesian coordinate frame. (See [3], for an example in development of robot tracking.) This controller is independent of the human dynamic behavior. The velocity controller is the lowest level of control that has been developed on the extender such that : 1) the extender is stabilized independent of the human dynamic behavior[1] and, 2) the final goal, which is to control the extender with one additional feedback loop can still be achieved. At this stage, it does not matter how good this controller is or how it has been developed, however, two variables generally affect the velocity of the velocity controlled extender: 1) the input velocity command to the extender, $u_e$ and, 2) the external force imposed on the extender, $f_e$. The tracking capability of the extender is a measure of how good the extender follows the input velocity commands, $u_e$. The reaction to external forces is another property of the extender which shows how the extender behaves under external forces[2]. Mapping $G_e$ and $S_e$ are given in equation 1 to show that, the extender velocity, $v_e$, is a function[3] of $u_e$ and $f_e$ (Subscript $_e$ stands for "extender").

$$v_e = G_e(u_e) + S_e(f_e) \qquad (1)$$

where:

$v_e$ = $n_e \times 1$ vector of extender velocity in a global cartesian coordinate frame,
$u_e$ = $n_e \times 1$ input velocity command,
$f_e$ = $n_e \times 1$ external force vector applied on the extender,

$G_e$ represents a stable mapping for the extender with the closed loop velocity controller. The extender will develop a velocity[4] in response to externally applied forces. In other words, the extender is not infinitely stiff to external forces. Even though the velocity controller for the extender can be designed so that the extender follows the input commands and rejects the disturbances, the extender velocity deviates "somewhat" in response to imposed forces. The extender velocity deviation is due to either structural compliance in the extender or the velocity controller compliance. The extender sensitivity function, $S_e$, is defined to map an externally applied force vector to the resulting extender velocity vector. If the extender is developed as a "good" velocity control system, the magnitude of the velocity which results from the application of an external force will be small.

Equality 1 is the most general mapping which describes the relationship between the extender trajectory and the input velocity command. (References [10], [11] give similar treatment for robot dynamic mdeling). For any type of velocity controller architecture (linear or nonlinear), one can

---

[1] It is of paramount importance in the safety of the human that the extender has a velocity controller as the lowest level of control. When the human is not in contact with the extender, the zero input to the velocity controller for the extender causes the extender to remain stationary.

[2] The external forces on the extender can be from the human or the object being manipulated. Here it is assumed that the extender is not constrained by another object. This analysis is concerned only with unconstrained maneuvering of the extender.

[3] The assumption that linear superposition holds for the effects of $f_e$ and $u_e$ is useful in understanding the nature of the interaction between the extender and human. This interaction is in a feedback form and will be clarified with the help of Figure 5. It will be described in Section 6, that the results of the nonlinear analysis do not depend on this assumption and one can extend the obtained results to cover the case when $G_e(u_e)$ and $S_e(f_e)$ do not superimpose.

[4] $v_e$ is not restrained to be the velocity of a particlur point on the extender.

always arrive at a particular function for $G_e$ and $S_e$. $G_e$ and $S_e$ are stable operators in the $L_p$ sense; $G_e : L_p^n \rightarrow L_p^n$, $S_e : L_p^n \rightarrow L_p^n$, and there exist scalars $\alpha_1$, $\alpha_2$, $\beta_1$, and $\beta_2$, such that the magnitude of the output velocity (commanded or external force response) is a linearly constrained function of the input (command or external force)[5], i.e.:

$$\| G_e[u_e] \|_p < \alpha_1 \| [u_e] \|_p + \beta_1 \tag{2}$$

$$\| S_e[d_e] \|_p < \alpha_2 \| [d_e] \|_p + \beta_2 \tag{3}$$

Defining stability in terms of $L_p$ sense is chosen because the structure of the mappings $G_h[\cdot]$ and $S_h[\cdot]$ are unspecified, and may be linear or nonlinear. We also desire to have $\int G_e[\cdot]dt$ be an $L_p$ stable function, i.e. there must be a limit on the position as well as the velocity of the extender. (This can be achieved by including a weak positioning loop in the design of $\int G_e[\cdot]dt$ ). The need for the $L_p$ stability of $\int G_e[\cdot]dt$ will become apparent in Section 6.

The extender dynamics can be represented in the frequency domain for linearly treated extenders[6]. The stable transfer function matrices, $G_e$ and $S_e$, are introduced to represent the tracking dynamics of a linearly treated extender.

$$v_e[j\omega] = G_e[j\omega]\, u_e[j\omega] + S_e[j\omega]\, f_e[j\omega] \tag{4}$$

Figure 1 represents the dynamic behavior of the extender. The operators in this block diagram are unspecified and may be frequency domain mappings or time domain input-output relationships.

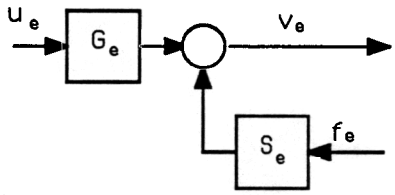


**Figure 1: Block Diagram of Extender Dynamics**

## 3. DYNAMIC BEHAVIOR OF THE HUMAN ARM

The modeling approach for human arm dynamics is similar to the one described for the extender. Depending on the type of maneuvering, the output of the human arm could be the position, the velocity or the contact force imposed by the human. For example, if a human pushes against an object, the contact force which develops can be regarded as an output. On the other hand, if the human approaches a particular point in space with his arm, then the position of his arm can be considered as an output. Along any of the directions in which the interaction (between the human arm and an object) takes place the human arm must take on the behavior of either an impedance or admittance [4, 5, and 9]. The impedance is defined as a mapping with a flow variable (e.g. velocity) as its input; and an admittance is defined as a mapping with an effort variable as its input. If the human arm's dynamic behavior is governed by an admittance (impedance), the object's dynamic behavior is governed by an impedance (admittance). In this analysis it is assumed that the human arm has an impedance property. In other words, the human assigns a trajectory in any interaction, rather than specifying the output force. Then the object with which the human is interacting determines the resulting interaction force.

With regard to the above assumption two variables affect the human arm trajectory: 1) the commanded trajectory issued from the human central nervous system, $u_h$ and, 2) the external force on the human arm imposed by the environment or the object being manipulated, $f_h$. Figure 2 shows the block diagram of the model of a human arm in a completely general form.

---

[5] The P-norm ($P \in [1,\infty]$) of a vector function, f, is defined as

$$\| f \|_p = \sum_{i=1}^{n} \| f_i \|_p^{\,2} \qquad \text{where} \quad \| f_i \|_p = \int_0^{\infty} |f_i|^p \, dt \qquad 1/2 \qquad 1/p$$

[6] Throughout this paper, for the benefit of clarity, the frequency domain theory has been developed in parallel with the nonlinear analysis for linearly treated robots.

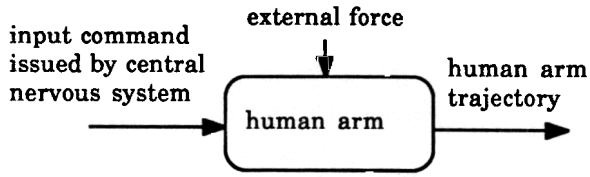


**Figure 2: The human arm trajectory is affected by both the input command and any externally applied force.**

The relationship between the input command and the human arm trajectory represents the tracking capability of the human arm. The relationship between the external force and the human arm trajectory represents the nature of the response of the human arm to external forces. In the most general form, the relationship between the inputs and outputs is given by equation 5. (Subscript $_h$ stands for "human").

$$y_h = G_h[u_h] + S_h[f_h] \tag{5}$$

where:

$y_h$ = $n_h \times 1$ vector of human arm position in a global cartesian coordinate frame,
$u_h$ = $n_h \times 1$ vector of intended position for the human arm generated by the central nervous system
$f_h$ = $n_h \times 1$ force vector applied on the human arm,

A nonlinear mapping, $G_h$, from the input command (which is issued by the central nervous system) to the human arm trajectory is defined to represent the tracking capability of the human arm. The closest we can come to understanding the input to this mapping is to know the state of the physical variables which we desire to achieve. For example, if the goal is to balance a broom, we know that the desired angle of deviation from the vertical must be zero degrees. The intent to balance the broom by maintaining an angle of zero degrees is defined as the input command for this mapping. Similarly, the closest we can come to understanding the output of the human arm is the observation of arm position or force applied in an interaction with the environment. An example of the output of the human arm would be the actual position of the human arm attained in attempting to balance the broom [8, 15]. The goal is to obtain a dynamic model that can represent the complete dynamic behavior of the human arm in a very general mathematical form. It is possible that there may be too many components in the human arm making analysis of rigid body dynamics not sufficient for modeling. This is an effort to avoid the structured dynamic models such as first or second order transfer functions to represent the dynamic behavior of the components of the human arm. These models are not general and the resulting simplified analysis develops non-general conclusions. Note that the physiological dynamic systems such as muscle contraction and nerve conduction delays are implicitly expressed in any part of this model. It is possible to experimentally measure the parameters which are involved in this model without explicitly determining the structured physiological dynamics which occur inside the mapping, $G_h$. Being that a human can position his arm in any position with arbitrary orientation, $n_h$=6.

Whenever an external force is applied to the human arm, the endpoint of the human arm will move in response. If the human arm is a "good" positioning system, the change in position due to the external force will be "small" as long as the magnitude of the external force lies within certain limits. The criterion for "small" and "good" in this context will be developed in this section. The sensitivity function $S_h$ is defined as a mapping from the $n_h \times 1$ externally applied force vector to the resulting $n_h \times 1$ position vector for the human arm. There is no restriction on the form of the mapping, $S_h$, it may be a linear or nonlinear. Also note that the structure of the mapping is not specified, just as in the mapping developed in equation 1. As stated above, for an arm with a good positioning system the deflection caused by the external force will be small for forces within certain limits.

In this model we are implicitly assuming that the human arm dynamics are stable operators in the $L_p$-sense. In other words, $G_h$ and $S_h$ are such that $G_h : L_p^n \rightarrow L_p^n$, $S_h : L_p^n \rightarrow L_p^n$, and there exist constants $\alpha_3$, $\alpha_4$, $\beta_3$, $\beta_4$, such that:

$$\| G_h[u_h] \|_p < \alpha_3 \| [u_h] \|_p + \beta_3 \tag{6}$$

$$\| S_h[f_h] \|_p < \alpha_4 \| [f_h] \|_p + \beta_4 \tag{7}$$

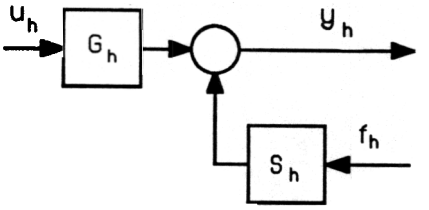


**Figure 3: Block Diagram Representation of Human Arm Dynamics**

In the linear domain, $G_h$ and $S_h$, operate as transfer function matrices which map the input trajectory amplitude to the output trajectory amplitude. Thus at any particular set of equilibrium angles, which are in the human range of motion the following frequency domain relationships hold:

$$y_h(j\omega) = G_h(j\omega)\, u_h(j\omega) + S_h(j\omega)\, f_h(j\omega) \tag{8}$$

The following block diagram in Figure 3 represents the model of the human arm. The structures of the mappings in this block diagram are completely unspecified. They may be defined in terms of frequency dependent transfer function matrices for a linear domain or a time domain nonlinear input-output relationship.

## 4. DYNAMICS OF THE EXTENDER AND HUMAN ARM TAKEN AS A WHOLE

If the extender and the human arm are in contact with each other, an interaction force will develop. The force developed by the interaction of the human arm and the extender will be modeled in terms of the relative positions of the extender and the human arm. The operator E is defined to map the difference in position, $y_h - y_e$ to the interaction force, $f_e$. The operator E represents the physical compliance of the human flesh and the force sensor which is located between the human arm and the extender. Note that since the force sensor is very stiff, E will be dominated by the physical compliance of the human arm flesh. Note that the force on the extender is equal in magnitude but opposite in direction to the force on the human arm. This relationship is expressed by equation 9.

$$f_e = -f_h = E(y_h - y_e) \tag{9}$$

where $y_e$ is the position of the extender. In a simple linear case, E can be modeled as the stiffness of a linear spring such that $f_e = E \times (y_h - y_e)$.

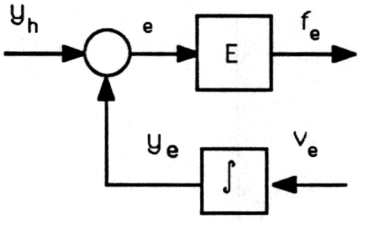


**Figure 4: The Interaction Between the Extender and the Human Operator**

An assumption is made so that this interaction is stable in the $L_p$ sense, that is, E: $L^n{}_p \rightarrow L^n{}_p$, and there exist scalars such that the interaction force is a linearly constrained function of the difference between the human arm position and the extender position, i.e.:

$$\| E(y_h - y_e) \|_p < \alpha_5 \| (y_h - y_e) \|_p + \beta_5 \tag{10}$$

When the extender and the human arm are in contact, equations 1, 5, 9, 10 are governing the dynamic behavior of the extender and human taken as a whole. These equations are written here in conjunction with equation 14 to form the four fundamental equations of the interaction between the human arm and the extender:

$$y_h = G_h(u_h) + S_h(f_h) \tag{11}$$
$$f_e = E(y_h - \int v_e \, dt) \tag{12}$$
$$v_e = G_e(u_e) + S_e(f_e) \tag{13}$$
$$f_h = -f_e \tag{14}$$

The interaction force acts on both the extender and the human arm and effects extender velocity and the human arm position as would an externally applied force. Note that the interaction force is defined as positive when $y_h - y_e > 0$, i.e. the human is pushing on the extender.

The block diagram shown in Figure 5 is a combination of the block diagrams shown in Figures 1, 3 and 4. Equations 11-14 represent the relationship of the mappings in Figure 5. Note that when the human arm and the extender are in contact, the number of degrees of freedom in the human arm is constrained to the number of degrees of freedom in the extender, i.e. $n_h = n_e$. When the human arm and the extender are not in contact, the interaction force becomes zero and the dynamics of the extender and human simplify to equations 1 and 5.

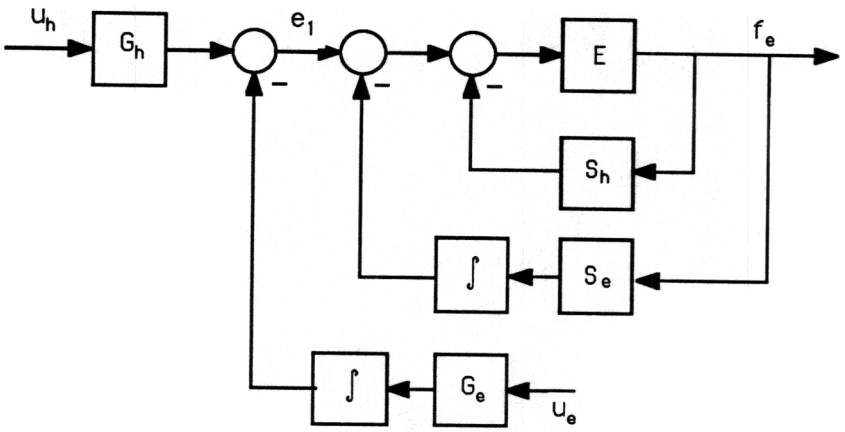


**Figure 5: Block Diagram of the Human and Extender**

The mapping $W: e_1 \rightarrow f_e$ is defined to simplify the block diagram of Figure 5. This mapping is shown in Figure 6.

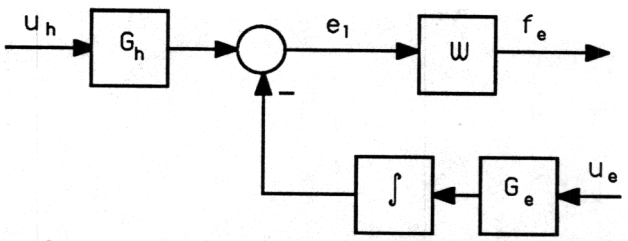


**Figure 6: Open loop mapping from desired hand position to the contact force.**

W is assumed to be a stable operator in the $L_p$ sense, that is $W: L_p^n \rightarrow L_p^n$, and there exist scalars $\alpha_6$ and $\beta_6$ such that the output is a linearly constrained function of the input :

$$\| W(e_1) \|_p < \alpha_6 \| (e_1) \|_p + \beta_6 \qquad (15)$$

If all the operators in Figure 6 are linear transfer function matrices, $v_e$ and $f_e$ are given by the following equations (when $u_e$ is zero):

$$v_e = S_e E (I_n + S_h E + S_e E/s)^{-1} G_h u_h \qquad (16)$$

$$f_e = E (I_n + S_h E + S_e E/s)^{-1} G_h u_h \qquad (17)$$

## 5. DESCRIPTION OF CLOSED LOOP ARCHITECTURE

As shown in Figure 5, the combination of the dynamics of the human and the extender, has two natural feedback loops. The first natural feedback loop involves the effect of the interaction force, $f_e$, on the extender. The interaction force has a small effect on the velocity of the extender if the extender velocity control loop has a small gain for the sensitivity function, $S_e$. The smaller the gain[7] of the extender sensitivity, the less effect this interaction force has on the extender velocity. The second natural feedback loop involves the effect of the same interaction force on the human arm. The human sensitivity function, $S_h$, is a mapping from the interaction force to the position of the human arm. A small value for the gain of $S_h$ results in a small deviation in the human's arm

[7] The smallest positive scalar constant $\alpha_4$ such that there exists a positive scalar constant $\beta_4$ such that inequality 7 is satisfied id defined as the gain of the operator, $S_e$.

position. Note that $S_h$ is a characteristic of the human arm dynamics. $S_h$ varies between humans and may vary within the same human. The sensitivity may vary as a result of several variables, one of which may be time.

If, in Figure 5 $u_e$ and $u_h$ are zero (i.e. the input to the extender is zero and the human has no intention to move) so the interaction force will be zero. If the human decides to move his hand (i.e. $u_h$ becomes a nonzero value), and $u_e$ is still set to zero, a small extender velocity will develop as a result of the interaction force. The deviation of the extender velocity will be trivial if $S_e$ has a small gain, even though the interaction force may not be small. In other words, the human arm generally does not have the strength to overcome the extender velocity control loop. We desire to increase the effective strength of the human by increasing the apparent sensitivity of the extender. This can be done by using the interaction force as an input to the extender velocity control loop as shown in Figure 7. The interaction force is measured, then filtered by the compensator, H. The compensator, H, is introduced to properly modify the interaction force. At this point there is no restriction being placed on the structure of H. The output of the compensator is then used as an extender input command, $u_e$. Note that the mapping $\int G_e H\{\cdot\}$ acts in parallel to $\int S_e$ and thus has the effect of increasing the apparent sensitivity of the extender. To increase the apparent sensitivity of the extender, Figure 7 suggests choosing a large gain for H. However, the designer does not have complete freedom in the design of H. The closed loop system must remain stable for any chosen value of H.

The goal is to develop a criterion on the compensator H which will guarantee the stability of the system in Figure 7. The compensator, H, must be designed to meet the specifications of the system in addition to satisfying the stability criterion. Using the Small Gain Theorem for the nonlinear input-output model of the system, a condition is obtained on the compensator, H, which will guarantee the stability of the closed loop system. The stability of the system is also analyzed via the multivariable Nyquist Criterion when the extender and the human arm are treated as linear time-invariant systems in the frequency domain. The frequency domain stability analysis gives more insight to the nature of the chosen architecture for the closed loop system.

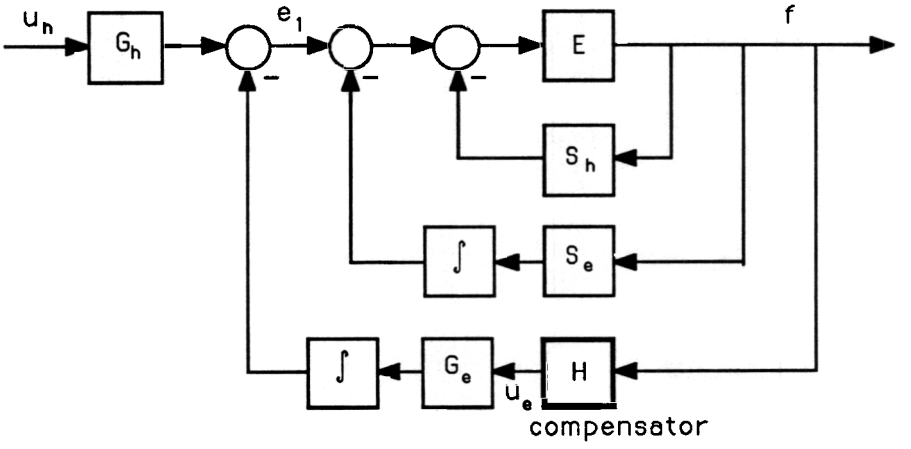


**Figure 7: Architecture of the Closed Loop System**

## 6. NONLINEAR TIME DOMAIN STABILITY ANALYSIS

A sufficient condition for stability of the closed loop system of Figure 7 is developed via the Small Gain Theorem. By determining this sufficient condition, a class of compensators will result which guarantee the stability of the closed loop system of Figure 7. Note that the stability condition derived in this section does not give any indication of the performance of the system; it only ensures a stable system. Section 9 will address the role of the compensator in system performance. The Small Gain Theorem is an appropriate approach in the stability analysis because unstructured and general operators are used in modeling the extender and human dynamic behavior. Figure 8 shows a simplified representation of the system in Figure 7. The operator W maps $e_1$ to the interaction force between the human and the extender, $f_e$. (If all the operators in the system are linear transfer function matrices, W is equivalent to $E[I_n + S_hE + S_eE/s]^{-1}$.

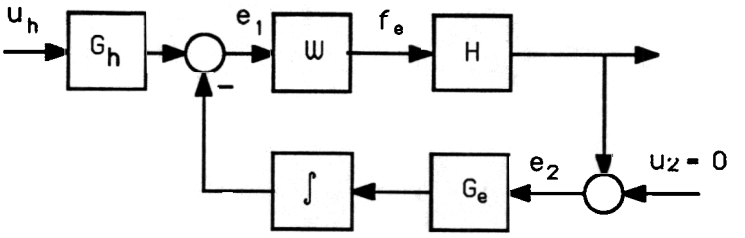


**Figure 8: Closed loop system, where H, $G_e$ and $G_h$ are unstructured mappings**

The following theorem (Small Gain Theorem), gives a sufficient condition to guarantee the stability of the closed loop system [1, 16].

Theorem:
If the following three conditions hold,

I. $\int G_e(e_2)$ is an $L_p$ stable operator, that is:

a) $\int G_e(e_2) : L^n_p \rightarrow L^n_p$ (18)

b) $\| \int G_e(e_2) \|_p < \alpha_7 \| e_2 \|_p + \beta_7$ ($\alpha_7$ and $\beta_7$ are positive constants) (19)

II. $H(\cdot)$ is selected as an $L_p$-stable operator such that the forward mapping $HW(e_1)$ remains $L_p$ stable, that is:

a) $HW(e_1) : L^n_p \rightarrow L^n_p$ (20)

b) $\|HW(e_1)\|_p < \alpha_8 \| e_1 \|_p + \beta_8$ ($\alpha_8$ and $\beta_8$ are positive constants) (21)

III. $\alpha_7 \alpha_8 < 1$ (22)

Then the closed loop system of Figure 8 is $L_p$ stable. The proof is given in Appendix A. Since $u_2$=0, $e_2$ is equal to $HW(e_1)$. Substituting for $\|e_2\|_p$ from inequality 21 into inequality 19 results in inequality 23.

$$\| \int G_e HW(e_1) \|_p < \alpha_7\alpha_8 \| e_1 \|_p + \alpha_7\beta_8 + \beta_7 \quad (23)$$

Inequality 23 shows that $\alpha_7\alpha_8$ represents the gain of the loop mapping, $\int G_e HW(e_1)$. Thus the third stability condition (22) requires that H be chosen such that the loop mapping, $\int G_e HW(e_1)$ is linearly bounded with less than unity slope. The following corollary develops a stability bound if H is selected as a linear transfer function matrix, while the other operators remain as nonlinear operators.

Corollary

If H and W are $L_p$ stable operators, and H is a linear operator, the following inequality is true[1]:

$$\| HW(e_1) \|_p \leq \gamma \| W(e_1) \|_p$$

where $\gamma = \sigma_{max}(M)$

$\sigma_{max}(\cdot)$ indicates the maximum singular value, and M is a matrix whose ijth entry is $\|H_{ij}\|_1$. In other words, each member of M is the $L_1$ norm of each corresponding member of H. Substituting from inequality 15 into 24:

$$\| HW(e_1) \|_p < \gamma\alpha_6 \| e_1 \|_p + \gamma\beta_6 \quad (26)$$

Since $u_2$ in Figure 8 is zero, inequality 26 can be substituted into inequality 19 to obtain inequality 27.

$$\| \int G_e HW(e_1) \|_p < \gamma\alpha_6\alpha_7 \| e_1 \|_p + \gamma\alpha_7\beta_6 + \beta_7 \quad (27)$$

In order to guarantee the closed loop stability of the system inequality 28 must be satisified:

$$\gamma\alpha_6\alpha_7 < 1 \quad (28)$$

$$\text{or } \gamma < \frac{1}{\alpha_6\alpha_7} \quad (29)$$

Note that inequality 29 is a sufficient condition to guarantee the stability of the system. If H is chosen such that $\gamma$ satisfies inequality 29, then the closed loop system is stable. If $\gamma$ does not satisfy inequality 29, no conclusion can be drawn as to the stability of the closed loop system of Figure 8.

## 7. FREQUENCY DOMAIN STABILITY ANALYSIS

This section develops a Nyquist stability criterion for the closed loop system in Figure 7 when all the operators are linear transfer function matrices [2, 12, and14]. The interaction force and the velocity of the extender are given by the following equations:

$$v_e = [S_e + G_eH]E[I_n + S_hE + S_eE/s + G_eHE/s]^{-1}G_hu_h \tag{30}$$

$$f_e = E[I_n + S_hE + S_eE/s + G_eHE/s]^{-1}G_hu_h \tag{31}$$

The objective is to arrive at a sufficient condition for the stability of the system. This condition leads to the introduction of a class of compensators that can be used to increase the apparent sensitivity of the extender system. The detailed derivation of the stability condition is given in Appendix B. According to the results of Appendix B, the sufficient condition for stability is given by inequality 32.

$$\sigma_{max}[G_eH/s] < \sigma_{min}([I_n + S_hE + S_eE/s]\,E^{-1}) \quad \text{for all} \quad \omega \in [0,\infty] \tag{32}$$

A more conservative condition is given by inequality 33:

$$\sigma_{max}[H] < \sigma_{min}[G_e^{-1}s[I_n + S_hE + S_eE/s]E^{-1}]$$
$$< \frac{1}{\sigma_{max}[G_e/s]\,\sigma_{max}[E[I_n + S_hE + S_eE/s]^{-1}]} \quad \text{for all} \quad \omega \in [0,\infty) \tag{33}$$

Inequality 33 is a sufficient condition for stability. If this inequality is not satisfied, no conclusion on the stability of the closed loop system can be reached. In other words, if H is chosen outside of this class, instability may occur. For a single degree of freedom extender, inequality 34 is a sufficient condition for stability.

$$|G_eH/s| < |[1 + S_hE + S_eE/s]^{-1}\,E| \quad \text{for all} \quad \omega \in [0,\infty) \tag{34}$$

## 8. COMPARISON OF STABILITY CONDITIONS

This section shows that the condition obtained via the Nyquist Criterion, (inequality 33) is a subclass of the condition obtained by the Small Gain Theorem. If all the operators in Figure 8 are linear transfer function matrices,

$$W[s] = E[I + S_hE + S_eE/s]^{-1} \tag{35}$$

Figure 9 shows the closed loop system when all the operators are linear transfer function matrices.

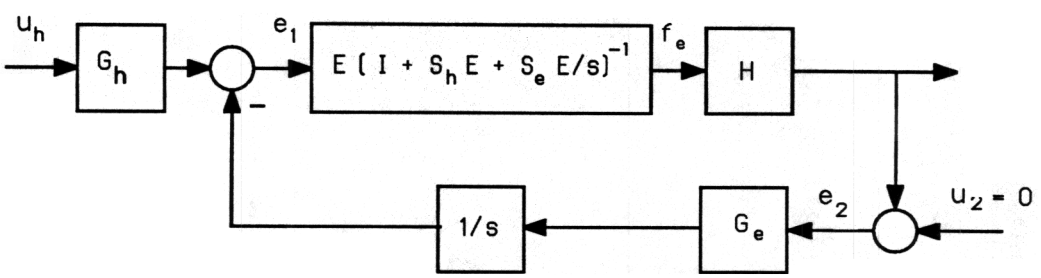


**Figure 9: Simplified Block Diagram of the Closed Loop System in the Frequency Domain**

The following inequalities are true for the linear system when p=2:

$$\| HW[e_1] \|_2 < \mu_1 \mu_3 \| e_1 \|_2 \tag{36}$$

$$\| \int G_e[e_2] \|_2 < \mu_2 \| e_2 \|_2 \tag{37}$$

where

$\mu_1 = \sigma_{max}[N_1]$, and $N_1$ is the matrix whose IJth entry is given by

$$[N_1]_{IJ} = \sup_\omega |[H[J\omega])_{IJ}|,$$

$\mu_2 = \sigma_{max}[N_2]$, and $N_2$ is the matrix whose IJth entry is given by

$$(N_2)_{ij} = \sup_\omega |(G_e(j\omega)/j\omega)_{ij}|$$

$\mu_3 = \sigma_{max}(N_3)$, and $N_3$ is the matrix whose ijth entry is given by
$(N_3)_{ij} = \sup_\omega |(W(j\omega))_{ij}|$ .

Considering inequalities 36 and 37, one can satisfy inequality 38 to guarantee the stability of the system.

$$\mu_1 \mu_2 \mu_3 < 1 \tag{38}$$

or:

$$\mu_1 < \frac{1}{\mu_2 \mu_3} \tag{39}$$

Note that the following are true:

$$\sigma_{max}(H) < \mu_1 \qquad \text{for all } \omega \in [0, \infty) \tag{40}$$

$$\sigma_{max}(G_e/s) < \mu_2 \qquad \text{for all } \omega \in [0, \infty) \tag{41}$$

$$\sigma_{max}(W) < \mu_3 \qquad \text{for all } \omega \in [0, \infty) \tag{42}$$

Substituting 40, 41 and 42 into inequality 39, which guarantees the stability of the nonlinear system, the following inequality is obtained:

$$\sigma_{max}(H) < \frac{1}{\sigma_{max}(G_e/s)\,\sigma_{max}(E(I + S_hE + S_eE/s)^{-1})} \quad \text{for all } \omega \in [0, \infty) \tag{43}$$

Inequality 43 is identical to inequality 33. This shows that the linear condition for stability given by the multivariable Nyquist Criterion is a subset of the general condition given by the Small Gain Theorem.

## 9. INTERPRETATION OF THE STABILITY CONDITION

In this section a physical interpretation of stability condition is developed. To develop this interpretation we use the linear stability condition given by inequality 32. Defining $S_t = E^{-1} + S_h$, inequality 32 can be rearranged to give inequality 44.

$$\sigma_{max}(G_eH/s) < \sigma_{min}(S_e/s + S_t) \quad \text{for all } \omega \in [0,\infty) \tag{44}$$

Note that $S_t$ is the total compliance of the human arm, i.e. the compliance of the flesh, $E^{-1}$, along with the positioning compliancy, $S_h$. Inequality 44 states that to guarantee stability of the closed loop system there must be some initial compliancy in either the human arm, $S_t$, or the extender velocity control system, $S_e$. If $S_e$ is very small, inequality 45 must be satisfied for stability:

$$\sigma_{max}(G_eH/s) < \sigma_{min}(S_t) \tag{45}$$

Inequality 45 states that the stability range will be larger if the total compliance of the human arm is large. A large value for $S_t$ implies a weak hand and/or soft tissue. A small $S_t$ results in a small stability range, and in the limit when $S_t \to 0$, no H can stabilize the closed loop system. A small value for $S_t$ implies a very good positioning system for the human arm, while a small value for $S_e/s$ represents a very good velocity tracking system for the extender. These two systems do not complement each other and may result in an unstable interaction. In the limiting case where $S_e$ is zero (i.e. the extender is a perfect velocity tracking system), $S_h$ is zero (i.e. human arm is a perfect positioning system) and $E \to \infty$ (the arm is very hard), no compensator H exists which will stabilize the system. The limiting case, where $S_e$, $S_h$ and $1/E$ are all zero, can also be represented as a violation of causality via the bond graph method [13].

By examining the ratio $\frac{|v_h|}{|v_e|}$ the effect of the compensator on system performance can be observed ($v_e \neq 0$). If this ratio approaches unity, then the extender velocity will approach the hand velocity. If all the operators in the closed loop system of Figure 7 are linear transfer function matrices, the relationship between the velocity of the human arm and the extender velocity is given by equation 46.

$$v_h = (I + s(S_eE + G_eHE)^{-1})v_e \tag{46}$$

The goal is to show that $v_e$ approaches $v_h$ as H becomes very large. The maximum ratio of the Euclidean norms of $v_h$ and $v_e$ is given by equation 47.

$$\max \frac{|v_h|}{|v_e|} = \sigma_{max}[I + s(S_eE + G_eHE)^{-1}]$$

or:

$$\max \frac{|v_h|}{|v_e|} \leq 1 + \frac{\sigma_{max}(sE^{-1})}{\sigma_{min}(G_e)\sigma_{min}(H) - \sigma_{min}(S_e)}$$

Within any bounded frequency range, the numerator of the fraction is bounded. $S_e$, $G_e$ and E are also bounded quantities. Thus if $\sigma_{min}(H) \rightarrow \infty$ the fractional portion of equation 48 will approach zero, and $\max \frac{|v_h|}{|ve|}$ will approach unity. Therefore, it is desirable to have a large gain for H in order to improve the performance of the system. However, we cannot make H arbitrarily large, because of the limitation imposed by the stability criterion (inequality 33). In other words, there is a trade-off between performance and stability in the closed loop system.

## 10. SUMMARY

Unstructured dynamic models for the human and extender have been developed in terms of nonlinear time domain mappings and linear transfer function matrices. The stability of the extender and human taken as a whole has been considered in this article. First, the Small Gain Theorem is used to determine a sufficient condition for stability in the completely general, unstructured, nonlinear system. Then, a sufficient condition for stability for the linear, time invariant, frequency domain model is determined. The condition for stability is determined using the multivariable Nyquist Criterion, with the "size" of the operators evaluated in terms of singular values. The equivalence of the conditions for stability when the Small Gain Theorem is extended to the linear system has been shown. The stability conditions can be given a physical interpretation which shows the limit on the gain of the compensator is dependent upon the total compliance in the system, i.e. the physical compliance of the flesh along with the sensitivities of the human arm and extender. The effect of compensation on system performance has also been shown. Based on this result it is desirable to have a large gain for the compensator. However, the stability condition places a limit on compensation and thus there is a trade off between performance and stability.

## APPENDIX A

Proof of the Stability Criterion:

First we define the closed loop mapping A, which maps from $u_h$ to $e_1$, $u_h$ and $e_2$. The goal is to determine under which condition this mapping will be stable. The error signals, $e_1$ and $e_2$ are given by equations A1 and A2.

$$e_1 = G_h(u_h) - \int G_e(e_2) \tag{A1}$$

$$e_2 = HW(e_1) \tag{A2}$$

For each finite time interval T, the following inequalities hold:

$$\| e_{1T} \|_p \leq \| G_h(u_h)_T \|_p + \| \int G_e(e_2)_T \|_p \quad \text{for all } t \in (0, T)$$

$$\| e_{2T} \|_p \leq \| HW(e_1)_T \|_p \quad \text{for all } t \in (0, T) \tag{A4}$$

Inequalities A3 and A4 are true because $\int G_e(e_2)$ and $HW(e_1)$ are $L_p$-stable. Also, since $\int G_e(e_2)$ and $HW(e_1)$ are $L_p$-stable operators, considering inequalities 19 and 21 inequalities A5 and A6 are true.

$$\| e_{1T} \|_p \leq \| G_h(u_h)_T \|_p + \alpha_7 \| e_{2T} \|_p + \beta_7 \quad \text{for all } t \in (0, T) \tag{A5}$$

$$\| e_{2T} \|_p \leq \alpha_8 \| e_{1T} \|_p + \beta_8 \quad \text{for all } t \in (0, T) \tag{A6}$$

Considering condition III (inequality 22), inequalities A7 and A8 can be obtained by rearranging inequalities A5 and A6.

$$\| e_{1T} \|_p < \frac{1}{1-\alpha_7\alpha_8}( \| G_h(u_h)_T \|_p + \beta_8 + \alpha_8\beta_7) \quad \text{for all } t\in[0, T] \quad (A7)$$

$$\| e_{2T} \|_p < \frac{1}{1-\alpha_7\alpha_8}(\alpha_7\| G_h(u_h)_T \|_p + \beta_7 + \alpha_7\beta_8) \quad \text{for all } t \in [0, T) \quad (A8)$$

Inequalities A3 and A4 show that $e_{1T}$, $e_{2T}$ are bounded for all $t < T$. This is true for every finite $T$, thus $e_1$ and $e_2$ are members of $L^n_{pe}$, or equivalently $A : L^n_{pe} \rightarrow L^n_{pe}$. In order to prove the $L_p$ stability of the closed loop system one must show that mapping A is an $L_p$ stable operator, as defined in Definition 5. Because the input $G_h(u_h) \in L^n_p$, by definition the p-norm of $G_h(u_h)$ will be less than $\infty$ for all $t \in [0, \infty)$. Combining this fact with inequalities A7 and A8, inequalities A9 and A10 are true.

$$\| e_1 \|_p < \infty \quad \text{for all } t \in [0, \infty)$$

$$\| e_2 \|_p < \infty \quad \text{for all } t \in [0, \infty) \quad (A10)$$

This inequality implies that $e_1$ and $e_2$ belong to $L_p$-space whenever $G_h(u_h)$ belongs to $L_p$-space. Now, by using the same steps taken to obtain inequalities A7 through A8, the following inequalities can be obtained (subscript $_T$ is dropped):

$$\| e_1 \|_p < \frac{1}{1-\alpha_7\alpha_8}( \| G_h(u_h) \|_p + \beta_8 + \alpha_8\beta_7) \quad \text{for all } t \in [0, \infty)$$

$$\| e_2 \|_p < \frac{1}{1-\alpha_7\alpha_8}(\alpha_7\| G_h(u_h) \|_p + \beta_7 + \alpha_7\beta_8) \quad \text{for all } t \in [0, \infty) \quad (A12)$$

Inequalities A11 and A12 show the linear boundedness of $\| e_1 \|_p$ and $\| e_2 \|_p$ by $\| G_h(u_h) \|_p$. Inequalities A9 - A12 taken together guarantee the $L_p$ stability of mapping A.

## APPENDIX B

The goal is to arrive at a sufficient condition to guarantee the stability of the closed loop system shown in Figure 7. We will use the multivariable Nyquist criterion to obtain this condition. The simplified block diagram of Figure 7 is shown in Figure B1.

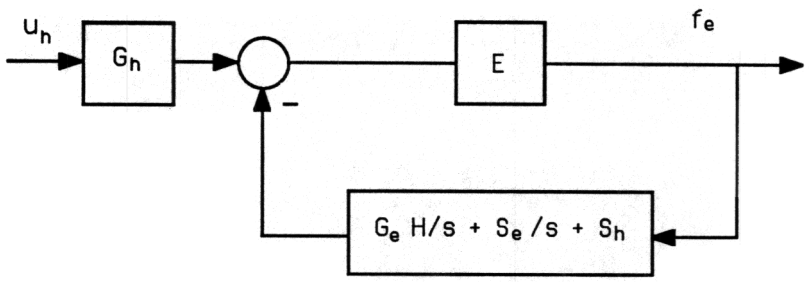


**Figure B1: Simplified Block Diagram of the Closed Loop System**

Note that there are three elements in the feedback loop. The transfer functions $S_h$ and $S_e/s$ represent the natural feedback loops which occur as a result of the interaction between the human and the extender. The third element, $G_eH/s$, is the controlled loop which acts to increase the apparent sensitivity of the extender. If we eliminate the feedback loop by setting $H = 0$, the system reduces to that represented by Figure 5, i.e. a human and extender in contact. The goal is to obtain a sufficient condition on the compensator which will guarantee the stability of the system when H is nonzero. To achieve this goal we use the multivariable Nyquist criterion. The following assumptions are made:

1. The closed loop system in Figure B1 is stable when $H = 0$. We are assuming that the system remains stable when the human and extender are in contact. This is the system shown in Figure 5.

2. H will be chosen as a stable linear transfer function matrix. If H is stable, the loop transfer function $[S_eE + S_hE/s + G_eHE/s]$ will have the same number of right half-plane poles as $[S_eE + S_hE/s]$.

3. The number of marginally stable poles for $[S_eE + S_hE/s + G_eHE/s]$ and $[S_eE + S_hE/s]$ are the same.

An assumption is made such that the system in Figure B1 is stable when $H = 0$. The goal is to determine how robust the system is when the term $G_eHE/s$ is added to the feedback loop. According to the Nyquist criterion, the system shown in Figure B1 will be stable as long as the number of clockwise encirclements of $\det[I + S_eE + S_hE/s + G_eHE/s]$ around the origin of the s-plane is equal to the number of unstable poles of the loop transfer function, $[S_eE + S_hE/s + G_eHE/s]$. By assumptions 2 and 3, we know that $[S_eE + S_hE/s + G_eHE/s]$ and $[S_eE + S_hE/s]$ have the same number of unstable or marginally stable poles. Assuming that the system is stable when $H = 0$; the number of encirclements of the origin by $\det[I + S_eE + S_hE/s]$ is equal to the number of unstable poles in $S_eE + S_hE/s$. When compensator H is added to the system, the number of encirclements of the origin by $\det[I + S_eE + S_hE/s + G_eHE/s]$ must be equal to the number of unstable poles in $S_eE + S_hE/s + G_eHE/s$ in order to guarantee closed loop stability. Because of the assumption that the number of unstable poles in $S_eE + S_hE/s$ and $(S_eE + S_hE/s + G_eHE/s]$ are identical, $\det[I + S_eE + S_hE/s + G_eHE/s]$ must have exactly the same number of encirclements of origin as $\det[I + S_eE + S_hE/s]$. In order to guarantee equal encirclements by $\det[I + S_eE + S_hE/s]$ and $\det[I + S_eE + S_hE/s + G_eHE/s]$, insurance is needed such that $\det[I + S_eE + S_hE/s + G_eHE/s]$ does not pass through the origin of the s-plane for all frequencies.

$$\det[I + S_eE + S_hE/s + G_eHE/s] \neq 0 \qquad \text{for all } \omega \in [0,\infty) \qquad \text{(B1)}$$

A sufficient condition which guarantees that $\det[ + S_eE + S_hE/s + G_eHE/s]$ does not pass through the origin of the s-plane is given by B2:

$$\sigma_{max}[G_eHE/s] < \sigma_{min}[I + S_eE + S_hE/s] \qquad \text{for all } \omega \in [0, \infty)$$

A more conservative condition:

$$\sigma_{max}[H] < \sigma_{min}[G_e^{-1}E^{-1}s + G_e^{-1}(S_e + S_h/s)] \qquad \text{for all } \omega \in [0, \infty)$$

## REFERENCES


1) Desoer, C.A., Vidyasagar, M., "Feedback Systems: Input-Output Properties", Academic Press, 1975.
2) Doyle, J.C., Stein, G., "Multivariable Feedback Desing: Concepts for a Classical/Modern Synthesis", IEEE Transactions on Automatic Control, Vol. AC26, No. 1, pp. 1-16, February 1981.
3) Ha, I. , Gilbert, E., "Robust Tracking in Nonlinear Systems and its Applications to Robotics", IEEE Conference on Robotics and Automation, San Francisco, April 1986.
4) Hogan, N., "Prostheses Should Have Adaptively Controllable Impedance", Proc. IFAC Symposium, Columbus, Ohio, May 1982.
5) Hogan, N., "Impedance Control: An Approach to Manipulation, Part 1: Theory, Part 2: Implementation, Part 3: Applications", ASME Journal of Dynamics Systems, Measurement, and Control, Vol. 107, No. 1, pp. 1-24, March 1985.
6) Hollerbach, J.M., "A Recursive Lagrangian Formulation of Manipulator Dynamics and a Comparative Study of Dynamics Formulation Complexity", IEEE Transactions on Systems, Man and Cybernetics Vol. SMC-10, No. 11, pp. 730-736, November, 1980.
7) Hollerbach, J.M., "Dynamic Scaling of Manipulator Trajectories", ASME Journal of Dynamic Systems, Measurement and Control, Vol. 106, pp.102-106, March 1984.
8) Johnsen, E.G. and Corliss, W.R. "Human Factors Applications in Teleoperator Design and Operation", Wiley Interscience.
9) Kazerooni, H., Houpt, P.K., Sheridan, T.B., "Fundamentals of Robust Compliant Motion for Manipulators", IEEE Journal of Robotics and Automation, Vol. 2, No. 2, June 1986.
10) Kazerooni, H., Tsay, T. I., "Stability Criteria for Robot Compliant Maneuvers", In proceeding of the IEEE International Conference on Robotics and Automation, Philadelphia, PA, April 1988.
11) Kazerooni, H., "Direct-Drive Active Compliant End Effector (Active RCC)", IEEE Journal on Robotics and Automation, Vol. 4, No. 3, June 1988.
12) Lehtomaki, N.A., Sandell, N.R., Athans, M., "Robustness Results in Linear-Quadratic Gaussian Based Multivariable Control Designs", IEEE Transactions on Automatic Control, Vol. AC-26, No. 1, pp. 75-92, February 1981.
13) Rosenberg R., Karnopp D., "System Dynamics: A Unified Approach", John Wiley, Sons, 1974.
14) Safonov, M.G., Athans, M., "Gain and Phase Margin for Multiloop LQG Regulators", IEEE Transactions on Automatic Control, Vol. AC-22, No. 2, pp. 173-179, April 1977.
15) Sheridan, T.B., Ferell, W.R., "Man-Machine Systems: Information, Control and Decision Models of Human Performance", MIT Press, Cambridge, Massachusetts, 1981.
16) Vidyasagar, M., "Nonlinear Systems Analysis", Prentice-Hall, 1978.